Korean J. Chem. Eng., **28**(4), 1126-1132 (2011)
DOI: 10.1007/s11814-010-0471-5

Efficient degradation of methylene blue dye by catalytic oxidation using the $Na_8Nb_6O_{19}\cdot 13H_2O/H_2O_2$ system

Chengtang Liu*,, Hui Xu**, Huaming Li*,†, Ling Liu**, Li Xu**, and Zhixiang Ye*****

*School of Chemistry and Chemical Engineering, Jiangsu University, Zhenjiang 212013, P. R. China
**School of the Environment, Jiangsu University, Zhenjiang 212013, P. R. China
***College of Resource and Environment, Chengdu University of Information Technology, Chengdu 610225, P. R. China
(*Received 15 September 2010 • accepted 3 November 2010*)

Abstract−$Na_8Nb_6O_{19}\cdot 13H_2O$ particles were synthesized by a simple hydrothermal method. The catalysts were characterized by X-ray diffraction (XRD), scanning electronic microscopy (SEM) and thermogravimetric and differential scanning (TG-DSC). The XRD and TG-DSC analyses indicated that $Na_8Nb_6O_{19}\cdot 13H_2O$ was an intermediate hexaniobate during the preparation of $NaNbO_3$ powders. Methylene blue (MB) dye degradation using $Na_8Nb_6O_{19}\cdot 13H_2O/H_2O_2$, Nb_2O_5/H_2O_2 and $NaNbO_3/H_2O_2$ systems were investigated, respectively. Among the catalytic oxidation systems, $Na_8Nb_6O_{19}\cdot 13H_2O$ showed the highest activity for degradation of MB in the presence of H_2O_2. The results indicated that the dye degradation efficiency could be 93.5% at 30 °C after 60 min in the presence of the $Na_8Nb_6O_{19}\cdot 13H_2O/H_2O_2$ system. It was also found that the degradation of MB over the catalytic systems followed pseudo-first-order kinetics, and the degradation rate was 0.02376 min^{-1} in the $Na_8Nb_6O_{19}\cdot 13H_2O/H_2O_2$ system, which was higher than that in the Nb_2O_5/H_2O_2 and $NaNbO_3/H_2O_2$ systems. A possible mechanism for MB catalytic oxidation degradation using the $Na_8Nb_6O_{19}\cdot 13H_2O/H_2O_2$ system was proposed.

Key words: $Na_8Nb_6O_{19}\cdot 13H_2O/H_2O_2$, Methylene Blue, Degradation

INTRODUCTION

Global environmental pollution and the relationship between environmental pollution and industrial activity, has become a more and more serious topic. Industries, such as cosmetics and synthetic detergents and dye manufacturing discharge toxic organic compounds that pollute the water. In recent years, dye wastewater, which is characterized by high concentration and complex composition, has attracted much more attention [1-3].

To treat the dye wastewater, various physical, chemical, and biological methods have been attempted. However, physical methods such as adsorption, ion-exchange or liquid-liquid extraction are ineffective on pollutants for they are so easily transferred to other organic pollutants, thus leading to secondary pollution. While the biological methods also have a number of disadvantages: special equipment and high operation costs are required, and the low speed of degradation limits the wide use of biological methods [4]. Advanced oxidation technique using highly reactive radicals, such as ·OH and O_2^-, is an excellent method for degradation of organic dye pollutants in water solution. In recent years, Fenton-type catalytic oxidation (Fe^{2+}/H_2O_2) using ·OH has been introduced into the degradation of the organic contaminants in wastewater. However, this process has disadvantages, such as low pH of the solution, the requirement of UV light and the amount of ferric hydroxide sludge [5,6]. To solve these issues, many materials have been presented: Fe/Fe_3O_4 [7], α-FeOOH [8], γ-FeOOH [9] and goethite, etc. [10]. These catalysts have proven to be useful in a wider pH range. However, many of them show low catalytic activity for degradation of organic contaminants. Therefore, it is necessary to explore a more efficient catalytic system. Currently, the synthesis of niobate powders has attracted much more attention for their ferroelectric, piezoelectric, and photocatalytic properties, especially their catalytic activity [11-22]. Batista et al. reported peroxomobium (V) complexes could catalyze the homogeneous oxidation of benzyl alcohol by H_2O_2 [23]. Passoni et al. prepared $Na_3[Nb(O_2)_4]\cdot 13H_2O$ and tested the $[Nb(O_2)_4]^{3-}$ anion for the oxidation of alcohols with H_2O_2 [24]. Compton investigated the $Ca_2Nb_3O_{10}$ nanosheets as catalysts for photochemical water splitting into hydrogen and hydrogen peroxide under UV irradiation [25]. Feliczak et al. showed that Nb-PMOs could offer new prospects on the application in catalysis in the presence of H_2O_2 [26]. Silva et al. reported Nb in the $Fe_{2-x}Nb_xO_3$ structure had a remarkable catalytic activity in the oxidation of organic contaminants under using H_2O_2 as an oxidant [27].

In the present work, the $Na_8Nb_6O_{19}\cdot 13H_2O$ nanoparticles were prepared by the hydrothermal method. Degradation of methylene blue (MB) dye using $Na_8Nb_6O_{19}\cdot 13H_2O/H_2O_2$, Nb_2O_5/H_2O_2 and $NaNbO_3/H_2O_2$ systems was comparatively investigated. The effects of calcinations and hydrothermal temperature and the reaction temperature of the solution on the MB degradation efficiency were studied. The kinetics of MB degradation was also investigated. Besides, the possible reaction mechanism for MB catalytic oxidation degradation by $Na_8Nb_6O_{19}\cdot 13H_2O/H_2O_2$ was discussed.

EXPERIMENTAL

1. Samples Preparation

Sodium hydroxide and Nb_2O_5 were the raw materials for the hy-

†To whom correspondence should be addressed.
E-mail: lihm@ujs.edu.cn

drothermal synthesis. In the synthesis procedure, 4.8 g sodium hydroxide was dissolved into 30 ml distilled water, and then the solution was mixed with 2.65 g Nb_2O_5. The above mixture was poured into an autoclave with the capacity of 100 ml. The autoclave was sealed and heated at various temperatures for 6 h. After being cooled, the resulting precipitate was centrifuged and washed with distilled water and absolute ethanol. Finally, the obtained product was dried at 60 °C for 5 h, and then the as-synthesized samples were calcined at different temperatures for 4 h.

2. Catalysts Characterization

The crystal structures of the synthesized powders were determined by X-ray powder diffraction on a Bruker D8 diffractometer with Cu Kα radiation (λ=1.5418 Å) in the range of 2θ=8-80°. The nanoparticle morphology was measured with a scanning electronic microscope (SEM, JEOL JSM-7001F). Thermogravimetric and differential scanning (TG-DSC) analysis were done on STA-449C Jupiter (NETZSCH Corporation, Germany).

3. Evaluation of Catalytic Activity: Degradation of MB

The oxidation of the MB dye (10 mg·L^{-1}) solution at pH 6.0 was carried out with a total volume of 150 mL and 20 mg of $Na_8Nb_6O_{19}\cdot 13H_2O$. To prevent the effect of thermal catalytic reaction, the temperature was kept at 30±1 °C. The suspension was first magnetically stirred for 30 min to ensure adsorption/desorption equilibrium and then H_2O_2 (32.5 mM·L^{-1}) was added to the solution. At set intervals, 5 mL suspension was taken from the reaction glass and analyzed after centrifugation. The catalytic degradation efficiency (E) of MB was obtained by the following formula:

$$E = \frac{C_0 - C}{C_0} \times 100\% = \frac{A_0 - A}{A_0} \times 100\% \quad (1)$$

Where C is the concentration of the MB solution at the time t, C_0 is the adsorption/desorption equilibrium concentration of MB, and A, A_0 is the corresponding values achieved by measuring the absorbance at 664 nm with UV-Vis spectrometry.

RESULTS AND DISCUSSION

1. Characterization of $Na_8Nb_6O_{19}\cdot 13H_2O$ Powders

Fig. 1 shows the XRD patterns of the products prepared under different reaction temperatures. It was found that when the hydrothermal temperature was enhanced to 120 °C (Fig. 1(b)), the Nb_2O_5 precursor (Fig. 1(a)) changed to $Na_8Nb_6O_{19}\cdot 13H_2O$ phase (JCPDS no. 14-0370). While at 140 °C, the mixture diffraction peaks of $Na_8Nb_6O_{19}\cdot 13H_2O$ and $NaNbO_3$ are present (Fig. 1(c)). However, when the temperature was up to 160 °C and 180 °C, the diffraction peaks of $Na_8Nb_6O_{19}\cdot 13H_2O$ could not be found, and there was only the $NaNbO_3$ phase (JCPDS no. 33-1270) (Fig. 1(d) and (e)). According to the XRD analysis, only $Na_8Nb_6O_{19}\cdot 13H_2O$ was formed at 120 °C, and 120 °C was the most suitable temperature to convert Nb_2O_5 to $Na_8Nb_6O_{19}\cdot 13H_2O$. The preparation process was shown as follows: $Nb_2O_5 \rightarrow Na_8Nb_6O_{19}\cdot 13H_2O \rightarrow NaNbO_3$, which was in accordance with Wu's reports [28]. The process of the $Nb_2O_5 \rightarrow Na_8Nb_6O_{19}\cdot 13H_2O \rightarrow NaNbO_3$ reaction may be conducted as follows : [28]

$$3Nb_2O_5 + 8OH^- \rightarrow Nb_6O_{19}^{8-} + 4H_2O \quad (2)$$

$$Nb_6O_{19}^{8-} + 8Na^+ + 13H_2O \rightarrow Na_8Nb_6O_{19}\cdot 13H_2O \downarrow \quad (3)$$

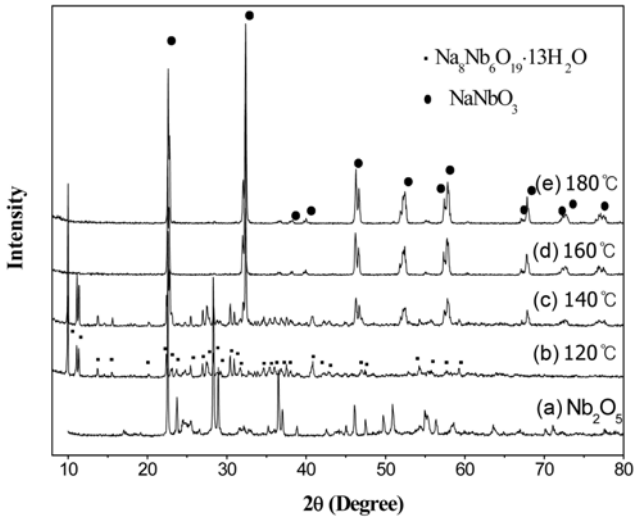

Fig. 1. XRD patterns of (a) Nb_2O_5 and the powders produced at different reaction temperatures for 6 h ((b) 120 °C, (c) 140 °C, (d) 160 °C, (e) 180 °C).

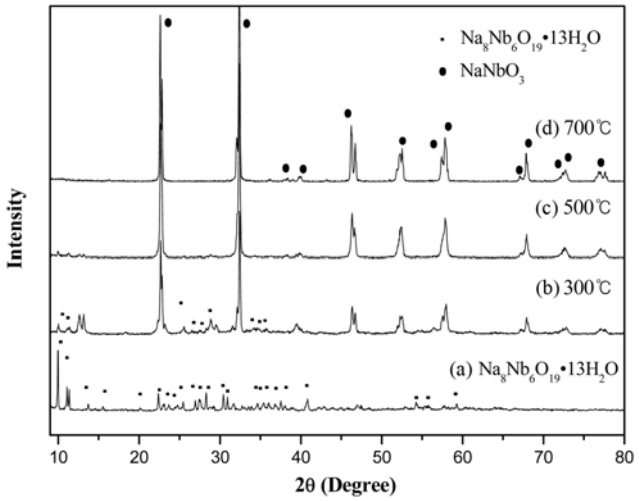

Fig. 2. XRD patterns of (a) $Na_8Nb_6O_{19}\cdot 13H_2O$ powder and the samples calcined at different temperatures for 4 h: (b) 300 °C, (c) 500 °C and (d) 700 °C.

$$Na_8Nb_6O_{19}\cdot 13H_2O \downarrow \rightarrow 6NaNbO_3 \downarrow + 2Na^+ + 2OH^- + 12H_2O \quad (4)$$

Fig. 2 shows the XRD patterns of the products obtained by calcining $Na_8Nb_6O_{19}\cdot 13H_2O$ at different temperatures. It can be seen that the products were a mixture of $Na_8Nb_6O_{19}\cdot 13H_2O$ with $NaNbO_3$ phases when the sample was calcined at 300 °C (Fig. 2(b)). However, with the increase of calcination temperature, the XRD pattern of $Na_8Nb_6O_{19}\cdot 13H_2O$ began to disappear gradually, while the pattern of $NaNbO_3$ became clear. When the calcined temperature was 500 °C and 700 °C (Fig. 2(c) and (d)), the diffraction peaks were well matched with the standard $NaNbO_3$ phase. As reported previously, $Nb_6O_{19}^{8-}$ ion whose edges were shared by NbO_6 octahedrons was easy to form the stable $NaNbO_3$ at the high temperatures during hydrothermal synthesis [28]. According to Fig. 2, the intermediate compound $Na_8Nb_6O_{19}\cdot 13H_2O$ is not stable, and it can be changed to the stable $NaNbO_3$ with the increase of calcination temperature.

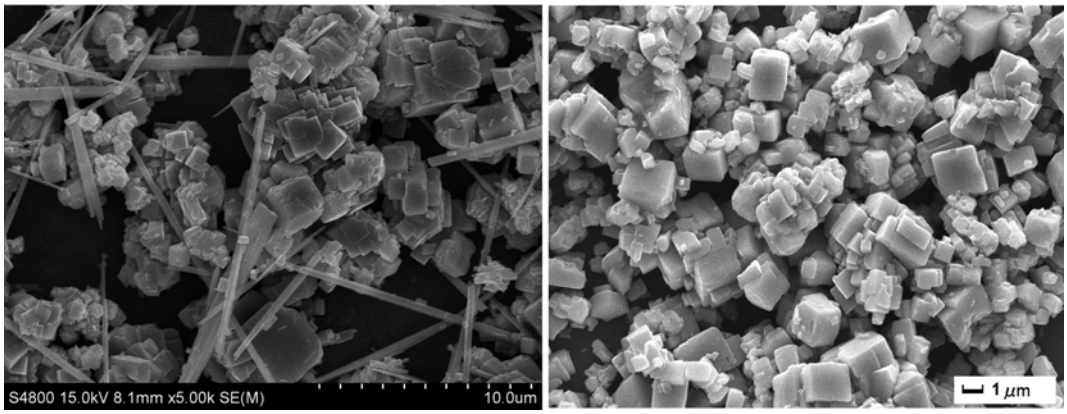

Fig. 3. The SEM images of the samples: (a) $Na_8Nb_6O_{19}\cdot13H_2O$; (b) $NaNbO_3$.

The SEM images of the samples in Fig. 3 illustrate the morphology evolution of the solid $Na_8Nb_6O_{19}\cdot13H_2O$ and $NaNbO_3$. Cubes and fibers can be observed in the $Na_8Nb_6O_{19}\cdot13H_2O$ samples (Fig. 3(a)). The fibers with the length of tens of micrometers and the width of hundreds of nanometers were observed (120 ºC). According to the XRD analysis (Fig. 1(b)), fibers and cubes of the product were attributed to the intermediate $Na_8Nb_6O_{19}\cdot13H_2O$ structure. However, homogeneous crystallization and morphology were difficult to achieve at the low temperature, because high sintering temperatures often cause serious volatilization of the alkali metal, which leads to stoichiometric variations in the sintered material [29]. As the reaction temperature was improved to 180 ºC, high purity niobate cubes were obtained (shown in Fig. 3(b)), and their XRD pattern (shown in Fig. 1(e)) suggested that there was only one crystal $NaNbO_3$ phase in this sample. Interestingly, the $Na_8Nb_6O_{19}\cdot13H_2O$ appeared as a metastable intermediate, and its crystallinity was easily transformed in the reaction process, which led to the formation of sodium niobate cubes [30].

TG-DSC analysis of $Na_8Nb_6O_{19}\cdot13H_2O$ is shown in Fig. 4. The endothermic peak in the DSC curve around 129.3 ºC was attributed to the decomposition of crystalline water of $Na_8Nb_6O_{19}\cdot13H_2O$ catalysts. It was found that the mass loss value of 18.49% was consistent with 18.8%, the theoretical value of crystalline water of $Na_8Nb_6O_{19}\cdot13H_2O$ catalysts. According to the XRD analysis (Fig. 2), the mass loss from 300 to 450 ºC was attributed to the phase transformation from $Na_8Nb_6O_{19}\cdot13H_2O$ to $NaNbO_3$. It also showed that $NaNbO_3$ cubes were more thermodynamically stable than the metastable intermediate $Na_8Nb_6O_{19}\cdot13H_2O$.

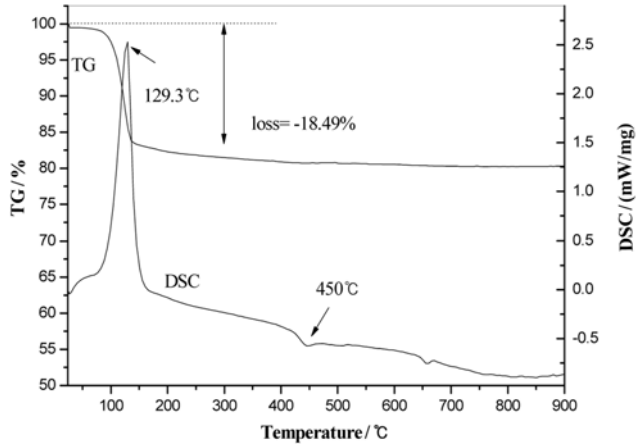

Fig. 4. TG-DSC curves of $Na_8Nb_6O_{19}\cdot13H_2O$ powders.

2. Degradation of MB

To investigate the catalytic activity of Nb_2O_5, $Na_8Nb_6O_{19}\cdot13H_2O$ and $NaNbO_3$ samples, the degradation activities of $Na_8Nb_6O_{19}\cdot13H_2O/H_2O_2$, Nb_2O_5/H_2O_2, $NaNbO_3/H_2O_2$ systems are shown in Fig. 5. It can be seen that in the absence of catalysts, there was no significant degradation of the MB solution in the case of H_2O_2. That is, H_2O_2 itself could not effectively induce degradation of MB dye. As for $Na_8Nb_6O_{19}\cdot13H_2O/H_2O_2$ system, MB degradation efficiency of 93.5% can be observed at 60 min. Compared with the MB degradation in $Na_8Nb_6O_{19}\cdot13H_2O/H_2O_2$ system, the dye degradation was significantly slow using Nb_2O_5 and $NaNbO_3$ samples. The results indicate that Nb_2O_5 and $NaNbO_3$ had no catalytic activity for MB degradation in the case of H_2O_2. Compared with other systems, such as the $Fe_{2-x}Nb_xO_3/H_2O_2$ system, the $Na_8Nb_6O_{19}\cdot13H_2O/H_2O_2$ system had higher catalytic activity for MB dye degradation [27]. In the $Na_8Nb_6O_{19}\cdot13H_2O/H_2O_2$ system, after the reaction time lasted

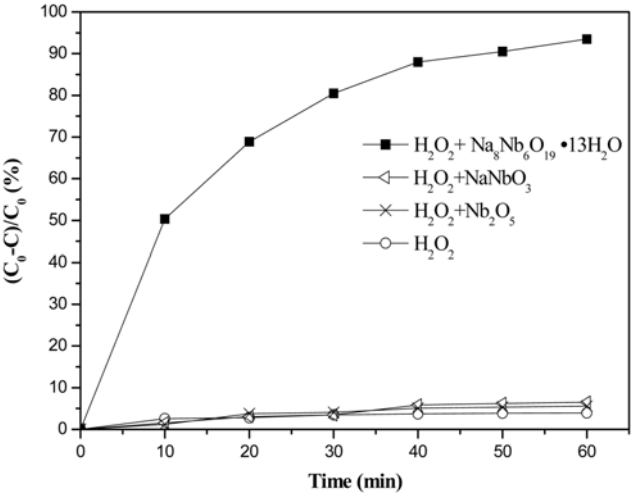

Fig. 5. The catalytic activity of different niobates with H_2O_2 (catalyst: 0.13 g·L^{-1}; H_2O_2: 32.5 mM·L^{-1}; MB: 10 mg·L^{-1}; T: 303 K).

30 min, ca. 90% of MB was degraded. However, in the $Fe_{2-x}Nb_xO_3/H_2O_2$ system, about 70% of MB was degraded in the same condition (60 min) [27].

The catalytic activity of the catalysts calcined at different temperatures is shown in Fig. 6. It was found that the calcination temperature had a negative effect on the catalytic activity. That was due to the appearance of $NaNbO_3$ phase when the calcination temperature was higher than 300 °C, which was confirmed in XRD analysis (Fig. 2). It was found that the catalysts calcined at 500 °C and 700 °C had nearly no catalytic activity. The catalytic activity of the sample decreased significantly with the increase of the calcination temperature.

However, the degradation process of MB with H_2O_2 was considerably dependent on the catalytic reaction temperature. Fig. 7 shows the effect of the reaction temperature (from 20 to be 50 °C) on the catalytic activity. In Fig. 7, it could be seen that the degrada-

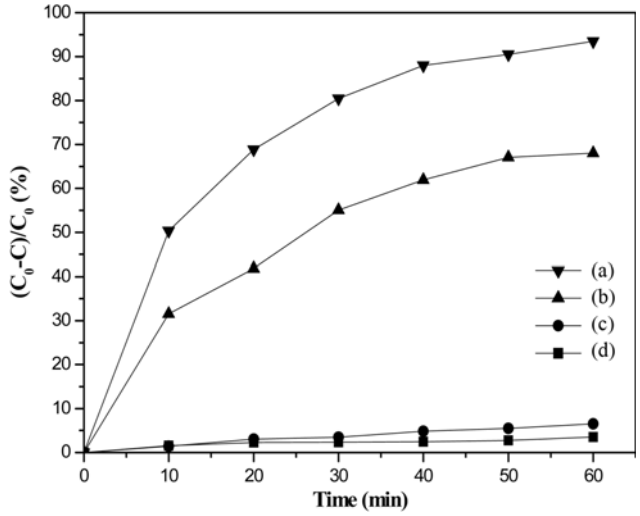

Fig. 6. Effect of catalysts calcined temperature on the reactions of MB degradation: (a) powders synthesized at 120 °C for 6 h and powders calcined at different temperatures for 4 h: (b) 300 °C, (c) 500 °C, (d) 700 °C (catalyst: 0.13 g·L^{-1}; H_2O_2: 32.5 mM·L^{-1}; MB: 10 mg·L^{-1}; T: 303 K).

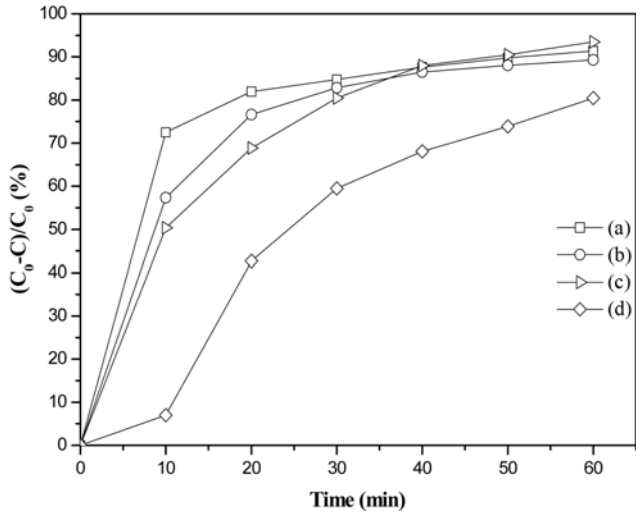

Fig. 7. Effect of reaction temperature on the degradation of MB: (a) 50 °C, (b) 40 °C, (c) 30 °C and (d) 20 °C (catalyst: 0.13 g·L^{-1}; H_2O_2: 32.5 mM·L^{-1}; MB: 10 mg·L^{-1}).

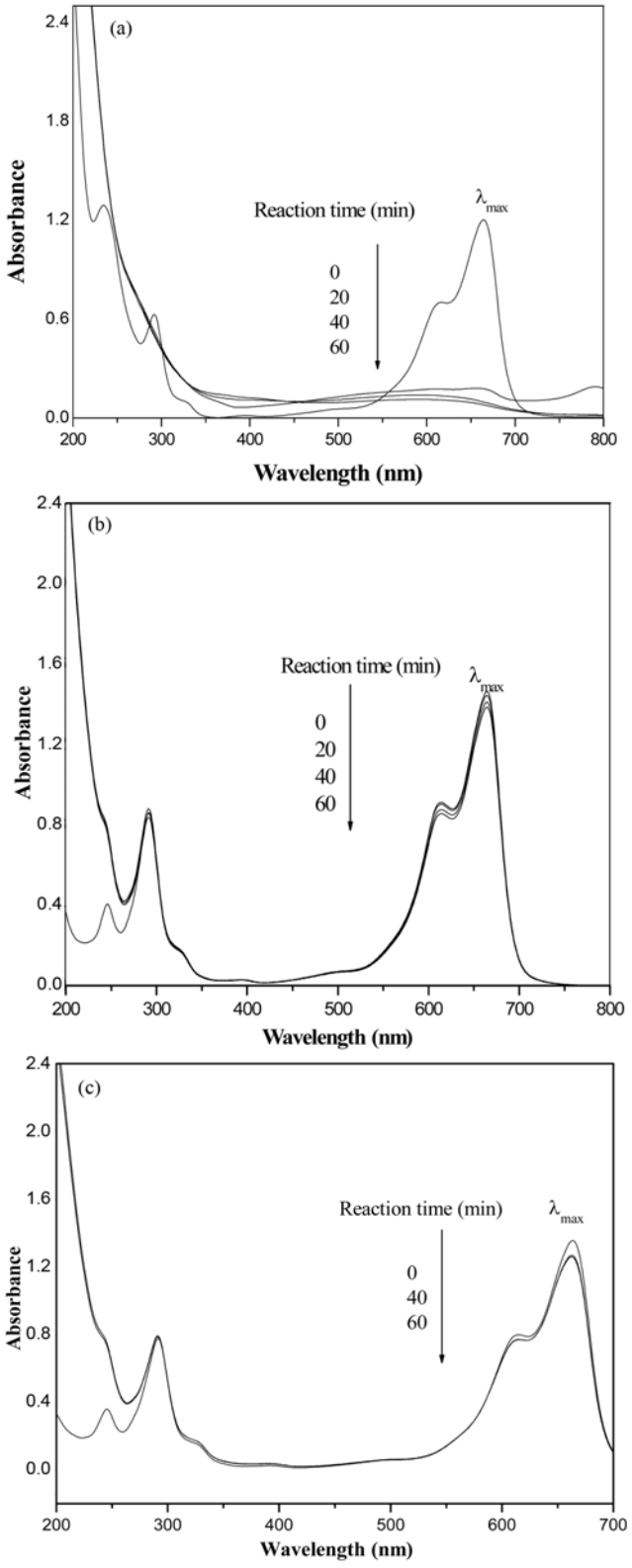

Fig. 8. The UV-vis spectral changes of MB of different niobate compounds systems: (a) $Na_8Nb_6O_{19}\cdot 13H_2O/H_2O_2$; (b) Nb_2O_5/H_2O_2; (c) $NaNbO_3/H_2O_2$ (catalyst: 0.13 g·L^{-1}; H_2O_2: 13 mM·L^{-1}; MB: 10 mg·L^{-1}; T: 303 K).

tion efficiency of MB under different temperature was enhanced with the increase of time. The degradation efficiency of MB increased remarkably from 6.9% (20 ºC) to 72.4% (40 ºC) in the initial 10 min. However, when the reaction temperature was up to 50 ºC, the degradation efficiency decreased from 93.5% (30 ºC) to 91.4% after 60 min. This may have been caused by the large decomposition of H_2O_2 at a high temperature. The results indicated that MB could be degraded at room temperature in short time.

The temporal evolution of the absorption spectral changes during the catalytic degradation of MB was monitored by UV-vis spectra (Fig. 8). Peaks at 235, 292, 620 and 664 nm correspond to the removal of MB [31]. During the reaction process, the characteristic absorption peak at 664 nm decreased dramatically and nearly disappeared after 60 min in the $Na_8Nb_6O_{19}\cdot13H_2O/H_2O_2$ system (Fig. 8(a)). The MB band at 207 nm was due to the absorption of H_2O_2 in the range of 185-300 nm [32]. It could also be found that the MB could not be sharply degraded in the case of Nb_2O_5/H_2O_2 or $NaNbO_3/H_2O_2$ system (Fig. 8(b) and 8(c)).

3. Kinetics

To investigate the kinetics of MB degradation over the Nb_2O_5, $Na_8Nb_6O_{19}\cdot13H_2O$ and $NaNbO_3$ in the presence of H_2O_2, a pseudo-first-order reaction model is introduced to describe the experimental data as follows:

$$-\ln(C/C_0)=k_{ap}t \quad (5)$$

where k_{ap} is the apparent rate constant, C_0 is the initial concentration of MB, t is the reaction time and C is the concentration of MB at the reaction time of t. Fig. 9 shows the kinetic curves for the decomposition of MB over Nb_2O_5, $Na_8Nb_6O_{19}\cdot13H_2O$ and $NaNbO_3$ samples (reaction temperature: 30 ºC). The kinetic parameters were calculated and listed in the inset table of Fig. 9. It appears that the degradation of MB by $Na_8Nb_6O_{19}\cdot13H_2O/H_2O_2$ followed the pseudo-first-order reaction kinetics. The apparent rate constants (k) of $Na_8Nb_6O_{19}\cdot13H_2O$, $NaNbO_3$ and Nb_2O_5 were found to be 0.02376, 6.1491×10^{-4}, 6.0720×10^{-4} min^{-1}. Evidently, the pseudo-first-rate kinetic constant of the degradation of MB with the assistance of the $Na_8Nb_6O_{19}\cdot13H_2O$ was significantly higher than that in the other catalytic systems (Nb_2O_5/H_2O_2 and $NaNbO_3/H_2O_2$).

The effect of reaction temperature on the MB degradation in aqueous solution in the presence of $Na_8Nb_6O_{19}\cdot13H_2O/H_2O_2$ system was investigated in the range of 20-50 ºC. It was generally accepted that the reaction temperature is a critical parameter determining the catalytic degradation reaction rate. It could be observed that when the reaction temperature was increased from 20 ºC to 50 ºC, the apparent degradation rate was increased (i.e., 0.0122-0.0271 min^{-1}). In Fig. 10, the correlation coefficient values (R) decreased gradually with the increase of reaction temperature. The result indicated that when the reaction temperature was lower, the correlation coefficient values (R) were higher than 0.99 (20-30 ºC). When the reaction temperature was increased to 50 ºC, the R value was 0.9053. Therefore, the degradation of MB by $Na_8Nb_6O_{19}\cdot13H_2O/H_2O_2$ does not fit the pseudo-first-order reaction model at the high reaction temperature (≥40 ºC).

4. The Proposed Catalytic Mechanism

To study the mechanism, the reaction of three niobate compounds (Nb_2O_5, $Na_8Nb_6O_{19}\cdot13H_2O$ and $NaNbO_3$) was carried out under the

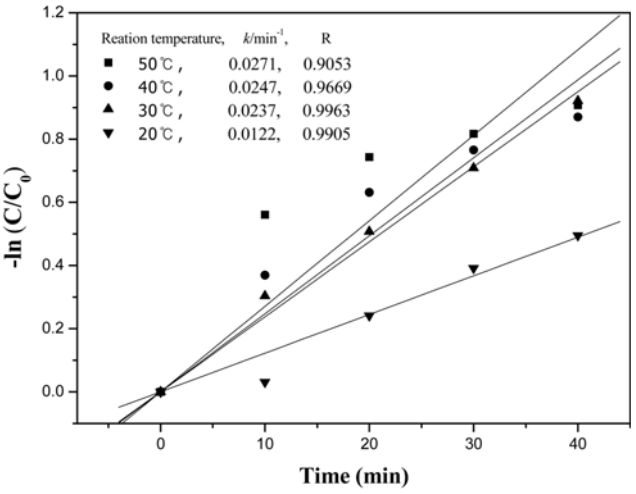

Fig. 10. Influence of reaction temperature on the degradation kinetics of MB by $Na_8Nb_6O_{19}\cdot13H_2O/H_2O_2$ system.

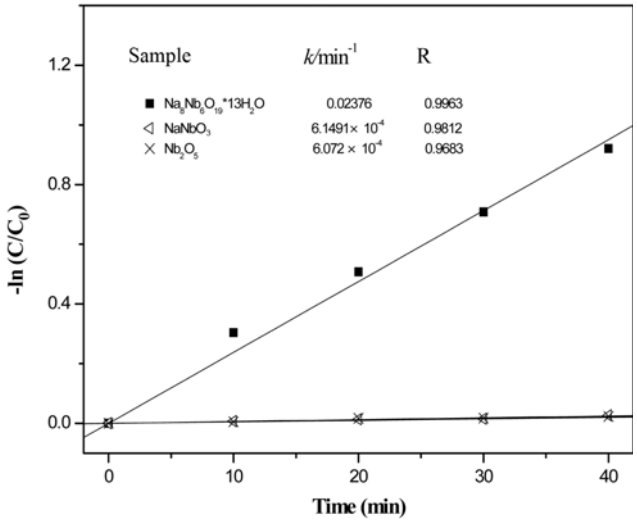

Fig. 9. Kinetics of MB degradation over Nb_2O_5, $Na_8Nb_6O_{19}\cdot13H_2O$ and $NaNbO_3$ particles in the presence of H_2O_2.

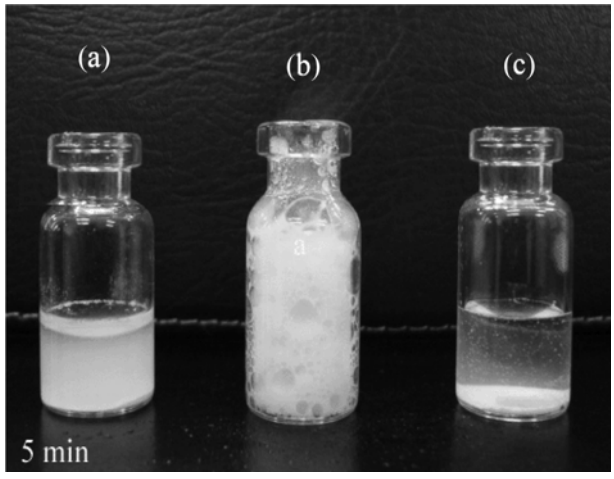

Fig. 11. Photos of different niobate compounds systems: (a) Nb_2O_5/H_2O_2; (b) $Na_8Nb_6O_{19}\cdot13H_2O/H_2O_2$; (c) $NaNbO_3/H_2O_2$.

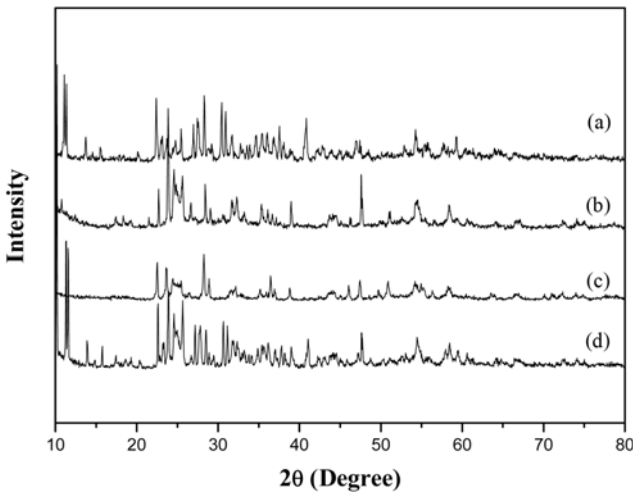

Fig. 12. X-ray diffraction patterns of powders: (a) $Na_8Nb_6O_{19}\cdot 13H_2O$ catalysts; (b) the products during the $Na_8Nb_6O_{19}\cdot 13H_2O/H_2O_2$ reaction system; (c) the Nb_2O_5 products after the $Na_8Nb_6O_{19}\cdot 13H_2O/H_2O_2$ reaction system; (d) the regenerated $Na_8Nb_6O_{19}\cdot 13H_2O$ catalyst.

same conditions. The reaction process of catalyst/H_2O_2 system is shown in Fig. 11. It was indicated that when Nb_2O_5 was added to the H_2O_2 solution, the reaction system could not generate many bubbles (Fig. 11(a)). The solution changed to the suspension as the $NaNbO_3$ compounds mixed with H_2O_2 in Fig. 11(c). It was also found that there was no dramatic reaction phenomenon as time went on. However, the $Na_8Nb_6O_{19}\cdot 13H_2O$ catalyst could react severely with H_2O_2 after five minutes in Fig. 11(b), and there were a large number of bubbles in the bottle following the intense reaction. It was also found that after two hours, in $Na_8Nb_6O_{19}\cdot 13H_2O/H_2O_2$ system, the pH increased significantly. The XRD patterns of $Na_8Nb_6O_{19}\cdot 13H_2O$ used during the oxidation reaction are shown in Fig. 12. It can be seen that the peak of $Na_8Nb_6O_{19}\cdot 13H_2O$ (Fig. 12(a)) was decreased in the reaction (Fig. 12(b)) and the phase of the product was Nb_2O_5 (Fig. 12(c)) after the reaction. The regenerated Nb_2O_5 powders with sodium hydroxide could synthesize new $Na_8Nb_6O_{19}\cdot 13H_2O$ material (Fig. 12(d)) by the hydrothermal method. Moreover, in the new $Na_8Nb_6O_{19}\cdot 13H_2O/H_2O_2$ system, the degradation efficiency (ca. 90% after 60 min) of MB solution did not exhibit significant decrease, indicating that the catalytic activity of the new $Na_8Nb_6O_{19}\cdot 13H_2O$ catalysts was still high during the reaction.

Similar to the Fenton-like reaction and the reaction of V (V) series compounds towards H_2O_2 [33-35], the activation of Nb (V) compound towards H_2O_2 may be as follows:

$$Nb^{5+}+H_2O_2 \rightarrow Nb^{4+}+\cdot OOH+H^+ \quad (6)$$

$$Nb^{5+}+\cdot OOH \rightarrow Nb^{4+}+H^++O_2 \quad (7)$$

$$Nb^{4+}+H_2O_2 \rightarrow Nb^{5+}+\cdot OH+OH^- \quad (8)$$

On the basis of the above results, the reaction mechanism is proposed: First, H_2O_2 was adsorbed on $Na_8Nb_6O_{19}\cdot 13H_2O$. H_2O_2 adsorbed on $Na_8Nb_6O_{19}\cdot 13H_2O$ was activated by transferring Nb^{5+} to Nb^{4+}, and ·OOH was produced, which was just like the reaction of V (V) compound towards H_2O_2. Then the reduced Nb^{4+} sites were oxidized by H_2O_2 to form the free radical ·OH. The molecular oxygen (according to Eq. (7)) contributed to the formation of Nb_2O_5; as reported previously, the reduced Nb^{4+} sites were oxidized to Nb^{5+} by the molecular oxygen [36]. Finally, the obtained Nb_2O_5 could synthesize $Na_8Nb_6O_{19}\cdot 13H_2O$ by hydrothermal method again. The formed free radical ·OH could participate in the MB degradation reaction. Therefore, the MB could be degraded by $Na_8Nb_6O_{19}\cdot 13H_2O/H_2O_2$ system in a short time.

CONCLUSION

$Na_8Nb_6O_{19}\cdot 13H_2O$ was an intermediate hexaniobate during preparing $NaNbO_3$ by a simple hydrothermal method ($Nb_2O_5 \rightarrow Na_8Nb_6O_{19}\cdot 13H_2O \rightarrow NaNbO_3$). The $Na_8Nb_6O_{19}\cdot 13H_2O$ was first tested and used as a highly-effective catalyst in the presence of H_2O_2. By comparing with Nb_2O_5/H_2O_2 system, $Na_8Nb_6O_{19}\cdot 13H_2O/H_2O_2$ system and $NaNbO_3/H_2O_2$ system, it was found that MB could be degraded most efficiently by $Na_8Nb_6O_{19}\cdot 13H_2O/H_2O_2$. The degradation of MB by $Na_8Nb_6O_{19}\cdot 13H_2O/H_2O_2$ followed the pseudo-first-order reaction kinetics and the degradation rate was 0.02376 min^{-1} in the case of $Na_8Nb_6O_{19}\cdot 13H_2O/H_2O_2$ system, which was higher than that in Nb_2O_5/H_2O_2 and $NaNbO_3/H_2O_2$ systems.

ACKNOWLEDGEMENTS

The authors genuinely appreciate the financial support of this work from the National Nature Science Foundation of China (No. 21007021 and 21076099) and the Doctoral Innovation Fund of Jiangsu (CX09B-210Z).

REFERENCES

1. M. S. Wong, W. C. Chu, D. S. Sun, H. S. Huang, J. H. Chen, P. J. Tsai, N. T. Lin, M. S. Yu, S. F. Hsu, S. L. Wang and H. H. Chang, *Appl. Environ. Microbiol*., **72**, 6111 (2006).
2. I. K. Konstantinou and T. A. Albanis, *Appl. Catal., B: Environ*., **49**, 1 (2004).
3. J. Tang, Z. Zou and J. Ye, *Chem. Mater*., **16**, 1644 (2004).
4. P. Baldrian, V. Merhautová, J. Gabriel, F. Nerud, P. Stopka, M. Hrubý and M. J. Benes, *Appl. Catal., B: Environ*., **66**, 258 (2006).
5. S. Karcher, A. Kornmuller and M. Jekel, *Water Res*., **36**, 4717 (2002).
6. A. H. Gemeay, I. A. Mansour, R. G. El-Sharkawy and A. B. Zaki, *J. Mol. Catal. A: Chem*., **193**, 109 (2003).
7. R. C. C. Costa, F. C. C. Moura, J. D. Ardisson, J. D. Fabris and R. M. Lago, *Appl. Catal., B: Environ*., **83**, 131 (2008).
8. J. Y. Feng, X. J. Hu, P. L. Yue, H. Y. Zhu and G. Q. Lu, *Water Res*., **37**, 3776 (2003).
9. S. Chou and C. Huang, *Chemosphere*, **38**, 2719 (1999).
10. W. F. de Souza, I. R. Guimarães, L. C. A. Oliveira, M. C. Guerreiro, A. L. N. Guarieiro and K. T. G. Carvalho, *J. Mol. Catal. A: Chem*., **278**, 145 (2007).
11. M. Nyman, T. M. Anderson and P. P. Provencio, *Cryst. Growth Des*., **9**, 1036 (2009).
12. I. P. Roof, S. Park, T. Vogt, V. Rassolov, M. D. Smith, S. Omar, J. Nino and H. C. zur Loye, *Chem. Mater*., **20**, 3327 (2008).
13. Q. P. Ding, Y. P. Yuan, X. Xiong, R. P. Li, H. B. Huang, Z. S. Li, T. Yu, Z. G. Zou and S. G. Yang, *J. Phys. Chem. C*, **112**, 18846 (2008).
14. H. Muthurajan, H. H. Kumar, V. Samuel, U. N. Gupta and V. Ravi,

Ceram. Int., **34**, 671 (2008).
15. G. Q. Li, T. Kako, D. F. Wang, Z. G. Zou and J. H. Ye, *J. Solid State Chem*., **180**, 2845 (2007).
16. Y. F. Chang, Z. P. Yang, X. L. Chao, Z. H. Liu and Z. L. Wang, *Mater. Chem. Phys*., **111**, 195 (2008).
17. E. Atamanik and V. Thangadurai, *J. Phys. Chem. C*, **113**, 4648 (2009).
18. J. T. Han, D. Q. Liu, S. H. Song, Y. Kim and J. B. Goodenough, *Chem. Mater*., **21**, 4753 (2009).
19. K. Katsumata, C. E. J. Cordonier, T. Shichi and A. Fujishima, *J. Am. Chem. Soc*., **131**, 3856 (2009).
20. T. Y. Ke, H. A. Chen, H. S. Sheu, J. W. Yeh, H. N. Lin, C. Y. Lee and H. T. Chiu, *J. Phys. Chem. C*, **112**, 8827 (2008).
21. C. D. Ling, M. Avdeev, R. Kutteh, V. V. Kharton, A. A. Yaremchenko, S. Fialkova, N. Sharma, R. B. Macquart, M. Hoelzel and M. Gutmann, *Chem. Mater*., **21**, 3853 (2009).
22. L. C. A. Oliveira, M. Gonçalves, M. C. Guerreiro, T. C. Ramalho, J. D. Fabris, M. C. Pereira and K. Sapag, *Appl. Catal., A: Gen*., **316**, 117 (2007).
23. D. Bayot, B. Tinant and M. Devillers, *Catal. Today*, **78**, 439 (2003).
24. L. C Passoni, M. R. H. Siddiqui, A. Steiner and I. Kozhevnikov, *J. Mol. Catal. A: Chem*., **153**, 103 (2000).
25. O. C. Compton and F. E. Osterloh, *J. Phys. Chem. C*, **113**, 479 (2009).
26. A. Feliczak, K. Walczak, A. Wawrzynczak and I. Nowak, *Catal. Today*, **140**, 23 (2009).
27. A. C. Silva, D. Q. L. Oloveira, L. C. A. Oliveira, A. S. Anastacio, T. C. Ramalho and J. H. Lopes, *Appl. Catal., A: Gen*., **357**, 79 (2009).
28. S. Y. Wu, W. Zhang and X. M. Chen, *J. Mater. Sci. Mater. Electron*., **21**, 450 (2010).
29. S. Lanfredi, L. Dessemond and A. C. Martins Rodrigues, *J. Eur. Ceram. Soc*., **20**, 983 (2000).
30. H. Zhu, Z. Zhen, X. Gao, Y. Huang, Z. Yan, J. Zou, H. Yin, Q. Zou, S. H. Kable, J. Zhao, Y. Xi, W. N. Martens and R. L. Frost, *J. Am. Chem. Soc*., **128**, 2373 (2006).
31. S. J. Yang, H. P. He, D. Q. Wu, D. Chen, X. L. Liang, Z. H. Qin, M. D. Fan, J. X. Zhu and P. Yuan, *Appl. Catal., B: Environ*., **89**, 527 (2009).
32. A. Lopez, A. Bozzi, G. Mascolo and J. Kiwi, *J. Photochem. Photobio., A: Chem*., **156**, 121 (2003).
33. J. Deng, J. Jiang, Y. Zhang, X. Lin, C. Du and Y. Xiong, *Appl. Catal., B: Environ*., **84**, 468 (2008).
34. Y. N. Kozlov, G. V. Nizova and G. B. Shul'pin, *J. Mol. Catal. A: Chem*., **227**, 247 (2005).
35. R. Z. Khaliullin, A. T. Bell and M. Head-Gordon, *J. Phys. Chem. B*, **109**, 17984 (2005).
36. T. Shishido, T. Miyatake, K. Teramura, Y. Hitomi, H. Yamashita and T. Tanaka, *J. Phys. Chem. C*, **113**, 18713 (2009).